PHYSICAL REVIEW D **79,** 034001 (2009)

Perturbative QCD predictions for two-photon exchange

Dmitry Borisyuk and Alexander Kobushkin

Bogolyubov Institute for Theoretical Physics, Metrologicheskaya street 14-B, 03680, Kiev, Ukraine

(Received 25 November 2008; published 4 February 2009)

We study two-photon exchange (TPE) in the elastic electron-nucleon scattering at high Q^2 in the framework of perturbative quantum chromodynamics. The obtained TPE amplitude is of order α/α_s with respect to Born approximation. Its shape and value are sensitive to the choice of nucleon wave function, thus study of TPE effects can provide important information about nucleon structure. With the wave functions based on quantum chromodynamics sum rules, TPE correction to the electron-proton cross section has a negative sign, is almost linear in ε, and grows logarithmically with Q^2 up to 7% at $Q^2 = 30$ GeV^2. The results of existing hadronic calculations, taking into account just the nucleon intermediate state, can be smoothly connected with the perturbative quantum chromodynamics result near $Q^2 \sim 3$ GeV^2. Above this point two methods disagree, which implies that the hadronic approach becomes inadequate at high Q^2. Other relevant observables, such as the electron/positron cross section ratio, are also discussed.

DOI: 10.1103/PhysRevD.79.034001 PACS numbers: 25.30.Bf, 12.38.Bx

I. INTRODUCTION

Two-photon exchange (TPE) in the electron-proton scattering has been actively discussed over the last several years. The impetus for this was initially given by the discovery of the so-called G_E/G_M problem in the proton form factor measurements [1]. It was shown later that the discrepancy between the Rosenbluth separation and polarization transfer methods can be at least partially eliminated after taking into account TPE effects [2]. Several experiments aimed at direct detection of TPE contribution to the cross section are proposed [3]. Nonzero single-spin asymmetry, which is induced by the imaginary part of TPE amplitude, was observed experimentally [4]. The role of TPE in the determination of the proton radius [5], parity-violating observables [6], and in deep inelastic scattering [7] was also discussed.

Currently, measurements of proton form factors at $Q^2 \sim 10$ GeV^2 are in progress [8] and other measurements in this region are proposed [9,10]. Clearly, these experiments call for a reliable estimate of TPE effects for high-Q^2 kinematics, which was one of the aims of the present work. At moderate Q^2, the TPE amplitude was calculated using nucleon and resonances as intermediate states (further called the hadronic approach) [2,11–13]. At high Q^2, however, a natural means for the description of any process involving hadrons and, in particular, TPE, is perturbative quantum chromodynamics (pQCD). Surprisingly, we have found no direct pQCD calculation of TPE in the literature.

In Ref. [14], TPE at high Q^2 was investigated using the formalism of generalized parton distributions. The authors doubt of pQCD applicability in the currently accessible kinematical region and thus use the alternative method. The values of TPE corrections obtained this way have the opposite sign to the results of the hadronic calculations. The authors also use an assumption that the most important diagrams are those in which both photons interact with the same quark. It turns out that in the pQCD approach the situation is reversed (see below, Sec. III B).

In the present paper we study TPE in the elastic electron-nucleon scattering at high Q^2 in the framework of pQCD. We employ the method, which was used to calculate baryon form factors in Refs. [15,16]. In the adopted approach, a nucleon with momentum p is represented as three collinearly moving quarks with momenta $x_i p$, where $0 < x_i < 1$, $\sum_{i=1}^{3} x_i = 1$. All quark masses and nucleon mass are neglected and thus $p^2 = (x_i p)^2 = 0$. The process amplitude has the form

$$\mathcal{M} = \langle \phi(y_i) | T(y_i, x_i) | \phi(x_i) \rangle, \tag{1}$$

where T is the hard scattering amplitude at quark level (represented by appropriate Feynman diagrams), and $\phi(x_i)$ and $\phi(y_i)$ are initial and final nucleon spin-flavor-coordinate wave functions (quark distribution amplitudes). The convolution with nucleon wave function implies a convolution of spinor indices and an integration over $dx_1 dx_2 dx_3 \delta(1 - x_1 - x_2 - x_3)$ and similarly for y_i.

To obtain a nonzero transition amplitude one must turn the momenta of all three quarks from the initial to final direction. In the one-photon exchange (Born) approximation one therefore needs at least two hard gluons to be exchanged between the quarks. It follows then that the amplitude scales as $\alpha\alpha_s^2/Q^6$ and the nucleon form factor—as α_s^2/Q^4. In the case of TPE the exchange of one gluon is sufficient and thus the leading-order pQCD contribution to the TPE amplitude should be $\sim\alpha^2\alpha_s/Q^6$. The ratio TPE/Born then will not be just α, as one may naively expect, but α/α_s, which is significantly larger and growing with Q^2. Thus the larger Q^2 is, the more important TPE will be.

The paper is organized as follows. In Sec. II the observables, affected by TPE, are discussed; Sec. III describes all ingredients of the calculation (hard scattering amplitude

for one-photon and two-photon exchange and nucleon wavefunctions); numerical results are given in Sec. IV; and conclusions—in Sec. V.

II. KINEMATICS AND OBSERVABLES

The momenta of particles are denoted according to $e(k) + N(p) \to e(k') + N(p')$. The transferred momentum is $q = p' - p$, $Q^2 = -q^2 > 0$ and $\nu = (p + k)(p' + k')$. The reduced cross section of the elastic electron-proton scattering can be written as

$$\sigma_R = \frac{Q^2}{4M^2}|\mathcal{G}_M|^2 + \varepsilon|\mathcal{G}_E|^2 + \frac{Q^2}{4M^2}\frac{\varepsilon(1-\varepsilon)}{1+\varepsilon}|\mathcal{G}_3|^2, \quad (2)$$

where M is proton mass, $\varepsilon = 1 - 2[1 + \nu^2/Q^2(4M^2 + Q^2)]^{-1}$, which for $Q^2 \gg M^2$ turns to

$$\varepsilon \approx (\nu^2 - Q^4)/(\nu^2 + Q^4), \quad (3)$$

and $\mathcal{G}_M$, $\mathcal{G}_E$, and $\mathcal{G}_3$ are certain invariant amplitudes (see details in Ref. [13]). In Born approximation $\mathcal{G}_E$ and $\mathcal{G}_M$ become usual electric and magnetic form factors and $\mathcal{G}_3$ vanishes, that is

$$\mathcal{G}_E = G_E + \delta\mathcal{G}_E, \qquad \mathcal{G}_M = G_M + \delta\mathcal{G}_M, \qquad \mathcal{G}_3 = \delta\mathcal{G}_3, \quad (4)$$

where prefix δ indicates TPE contribution. The dominant part of the cross section at high Q^2 comes from the generalized magnetic form factor $\mathcal{G}_M$ and looks like

$$\sigma_R \approx \frac{Q^2}{4M^2}G_M^2\left(1 + 2\,\mathrm{Re}\frac{\delta\mathcal{G}_M}{G_M}\right). \quad (5)$$

Hence we should primarily study TPE contribution $\delta\mathcal{G}_M$. This quantity also defines the positron/electron elastic cross section ratio

$$R = \frac{\sigma^+}{\sigma^-} = \left|\frac{G_M - \delta\mathcal{G}_M}{G_M + \delta\mathcal{G}_M}\right|^2 \approx 1 - 4\,\mathrm{Re}\frac{\delta\mathcal{G}_M}{G_M}. \quad (6)$$

The generalized electric form factor $\mathcal{G}_E$ is suppressed in the cross section by $M^2/Q^2 \ll 1$. Therefore a consideration of TPE corrections to $\mathcal{G}_E$ makes little sense.

The amplitude $\delta\mathcal{G}_3$ in principle can be measured in polarization experiments. Namely, neglecting terms of order M^2/Q^2, the polarization of the final proton in the recoil polarization method is purely longitudinal and equals

$$P_\ell = h\sqrt{1-\varepsilon^2}\left(1 - \frac{2\varepsilon^2}{1+\varepsilon}\,\mathrm{Re}\frac{\delta\mathcal{G}_3}{G_M}\right), \quad (7)$$

where h is electron helicity. Thus a precise study of ε dependence of P_ℓ may give an access to $\delta\mathcal{G}_3$.

III. AMPLITUDE CALCULATION

A. One-photon exchange

First, we briefly review the pQCD calculation of form factors [15,16].

The nucleon form factors, or the elastic electron-nucleon scattering in one-photon exchange approximation, is described in pQCD to leading order in α_s by seven diagrams (Fig. 1(a)). For example, the piece of amplitude, coming from the first of them, is

$$\mathcal{M} = -\frac{4\pi\alpha}{q^2}\left(\frac{4\pi\alpha_s}{q^2}\right)^2 \cdot 6 \cdot (4/9) \cdot (-q^2)\bar{u}'\gamma_\mu u\langle\phi(y_i)|e_1\frac{\gamma_\alpha(y_1\hat{p}' + y_2\hat{p}' - x_2\hat{p})\gamma_\beta(x_1\hat{p} + \hat{q})\gamma_\mu \otimes \gamma_\alpha \otimes \gamma_\beta}{x_2^2 y_2 x_3 y_3(y_1 + y_2)(1 - x_1)q^4}|\phi(x_i)\rangle, \quad (8)$$

where u and u' are electron spinors, the overall minus sign is due to the *negative* electron charge, e_i is the ith quark charge, $6 = 3!$ is a symmetry factor due to possible permutations of quark lines, and $(-q^2)$ comes from quark and nucleon spinors normalization,

$$4/9 = \left\langle\frac{1}{2}\lambda^a\frac{1}{2}\lambda^b \otimes \frac{1}{2}\lambda^a \otimes \frac{1}{2}\lambda^b\right\rangle \quad (9)$$

is a color factor (here λ^a are Gell-Mann matrices and $\langle\,\rangle$ means averaging over totally antisymmetric color wave function). In the last equation as well as in Eq. (8) we separate matrices, acting on different quarks, by the $\otimes$ sign. Thus in the expression for the color factor $\frac{1}{2}\lambda^a\frac{1}{2}\lambda^b$ acts on the first, $\frac{1}{2}\lambda^a$ on the second, and $\frac{1}{2}\lambda^b$ on the third quark.

Adding up contributions from all the diagrams and using the fact that spin-flavor-coordinate wave function is totally symmetric under quark interchange, we obtain

$$\mathcal{M} = \frac{4\pi\alpha}{Q^2}\bar{u}'\gamma_\mu u\bar{U}'\gamma_\mu U \cdot G_M(q^2), \quad (10)$$

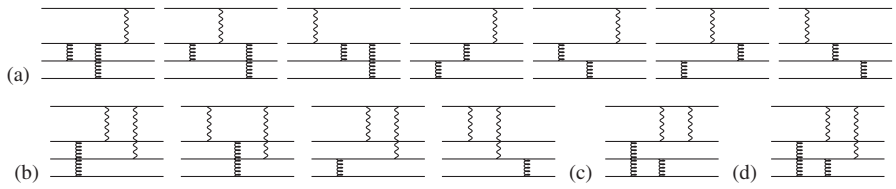

FIG. 1. pQCD diagrams for $eN \to eN$: one-photon exchange (a), two-photon exchange, leading order (b), subleading order (c, d).

where U and U' are initial and final nucleon spinors and

$$G_M = \frac{16}{3}\left(\frac{4\pi\alpha_s}{q^2}\right)^2 \langle\phi(y_i)|(1+h_1h_3)\left\{\frac{2e_1}{x_3y_3(1-x_1)^2(1-y_1)^2}+\frac{2e_1}{x_2y_2(1-x_1)^2(1-y_1)^2}+\frac{e_2}{x_1y_1x_3y_3(1-x_1)(1-y_3)}\right.$$
$$\left.-\frac{e_1}{x_2y_2x_3y_3(1-x_1)(1-y_3)}-\frac{e_1}{x_2y_2x_3y_3(1-x_3)(1-y_1)}\right\}|\phi(x_i)\rangle, \tag{11}$$

where $h_i = \pm 1$ are signs of quark helicities; the helicities of initial and final quarks should be equal. This is equivalent to the well-known result [15,16].

B. Two-photon exchange

For the case of TPE, there are only four distinct diagrams in the leading order (Fig. 1(b)) in which the photons are connected to different quarks. The diagrams in which both photons interact with the same quark (Fig. 1(c)) need one more gluon to turn all quarks' momenta and thus are subleading in α_s. Moreover, the evaluation of such diagrams alone is inconsistent, since the contribution of the same order in α_s comes from one-gluon corrections to the leading diagrams (e.g. Fig. 1(d)).

One point needs to be clarified here. If we remove the electron line, the diagrams (Fig. 1(b)–1(d)) will represent Compton scattering of virtual photons on the nucleon [doubly virtual Compton scattering (VVCS)]. And vice versa, TPE can be viewed as a process in which the virtual photon, emitted by the electron, is scattered from the proton and then absorbed back by the electron. VVCS has an important qualitative difference from the well-studied *real* Compton scattering (RCS). Since the momentum r of the real photon satisfies $r^2 = 0$, it cannot alone turn the quark's momentum: $(x_ip - y_ip')^2 \neq 0 = r^2$. Therefore diagrams with the structure like Fig. 1(b) vanish for RCS, and the amplitude expansion begins with $O(\alpha_s^2)$ terms (diagrams like Fig. 1(c) and 1(d)). On the contrary, in the case of VVCS the photons may be highly virtual, diagrams Fig. 1(b) contribute, and leading terms in VVCS amplitude are $O(\alpha_s)$. Hence, one cannot employ an analogy with RCS in the analysis of TPE (cf. Ref. [14]). We write down the expression for the first diagram in Fig. 1(b), the rest are analogous. We have

$$\delta\mathcal{M} = \left(\frac{4\pi\alpha}{q^2}\right)^2 \frac{4\pi\alpha_s}{q^2}\cdot 6\cdot(-2/3)\cdot(-q^2)$$
$$\times\langle\phi(y_i)|e_1e_2\frac{\bar{u}'\gamma_\mu(\hat{k}+x_2\hat{p}-y_2\hat{p}')\gamma_\nu u}{(k+x_2p-y_2p')^2+i0}$$
$$\times\frac{\gamma_\alpha(y_1\hat{p}'+y_3\hat{p}'-x_3\hat{p})\gamma_\mu\otimes\gamma_\nu\otimes\gamma_\alpha}{x_2y_2x_3^2y_3(x_1+x_3)(y_1+y_3)^2q^2}|\phi(x_i)\rangle, \tag{12}$$

where the color factor is $-2/3 = \langle\frac{1}{2}\lambda^a\otimes\frac{1}{2}\lambda^a\otimes 1\rangle$. After some algebraic transformations and using wave function symmetry, we obtain the full TPE amplitude in the form

$$\delta\mathcal{M} = \frac{4\pi\alpha}{Q^2}\bar{u}'\gamma_\mu u\bar{U}'\gamma_\nu U\left(\frac{4p_\mu k_\nu}{\nu}\delta\mathcal{G}_3 + g_{\mu\nu}\delta G_M\right), \tag{13}$$

where

$$\delta G_M = -\frac{256\pi^2\alpha\alpha_s}{q^4}\langle\phi(y_i)|\frac{e_1e_2(1-h_1h_3)}{x_2y_2x_3y_3(1-x_2)(1-y_2)}$$
$$\times\frac{(\nu-q^2)/(1-x_2)+(\nu+q^2)/(1-y_2)-2\nu}{\nu(x_2-y_2)-q^2(x_2+y_2-2x_2y_2)+i0}$$
$$\times|\phi(x_i)\rangle, \tag{14}$$

$$\delta\mathcal{G}_3 = -\frac{256\pi^2\alpha\alpha_s}{q^4}\langle\phi(y_i)|\frac{e_1e_2(1-h_1h_3)}{x_2y_2x_3y_3(1-x_2)(1-y_2)}$$
$$\times\frac{2\nu}{\nu(x_2-y_2)-q^2(x_2+y_2-2x_2y_2)+i0}|\phi(x_i)\rangle. \tag{15}$$

From this expression it is easy to see the crossing symmetry of TPE amplitudes δG_M and $\delta\mathcal{G}_3$: both are ν-odd. The quantity $\delta\mathcal{G}_M$, associated with the cross section correction (5), equals [13]

$$\delta\mathcal{G}_M = \delta G_M + \varepsilon\delta\mathcal{G}_3. \tag{16}$$

As implied by Eqs. (5)–(7), it is better to consider ratios $\delta\mathcal{G}_M/G_M$ and $\delta\mathcal{G}_3/G_M$ than the amplitudes themselves. This way we also avoid the uncertainty related with the absolute normalization of nucleon wave functions, since it cancels in the ratio. We have

$$\left(\frac{\delta G_M}{G_M},\frac{\delta\mathcal{G}_3}{G_M}\right) = -\frac{3\alpha}{\alpha_s}\frac{\langle\phi(y_i)|(T_{\delta G_M},T_{\delta\mathcal{G}_3})|\phi(x_i)\rangle}{\langle\phi(y_i)|T_{G_M}|\phi(x_i)\rangle}, \tag{17}$$

where T_{G_M}, $T_{\delta G_M}$, and $T_{\delta\mathcal{G}_3}$ are the expressions, sandwiched between wave functions in Eqs. (11), (14), and (15).

The obtained TPE amplitudes are free from infrared (IR) divergence. This becomes clear if we recall that the IR-divergent terms are proportional to the Born amplitude. Thus $\delta\mathcal{G}_3$ is IR-finite (it vanishes in the Born approximation), and

$$\delta G_M^{(\mathrm{IR})} \sim \alpha G_M \ln\lambda^2, \tag{18}$$

where λ is an infinitesimal photon mass. The magnetic form factor (11) is a quantity of order $O(\alpha_s^2)$. On the other hand, the leading-order contribution to TPE is $O(\alpha_s)$ and

therefore IR divergence should only appear as a *subleading* effect, in the next order in α_s.

Another interesting point pertains to photons' virtualities. In all diagrams they are both of order Q^2, e.g. in the first diagram $q_1^2 = -x_2 y_2 Q^2$ and $q_2^2 = -(x_1 + x_3) \times (y_1 + y_3) Q^2$. We may conclude that the leading contribution to the amplitude at high Q^2 comes from the region where both photons are hard, $q_1^2 \sim q_2^2 \sim -Q^2$.

C. Wave functions

Before turning to numerical calculations, we must specify a model for wave functions. The requirement for the total spin and isospin to be $1/2$ together with the Pauli principle fixes the following form of the quark distribution amplitude (for the proton of positive helicity):

$$|\phi(x_i)\rangle = \frac{f_N}{\sqrt{6}} \phi_1(x_1, x_2, x_3)(|u_\uparrow u_\downarrow d_\uparrow\rangle - |u_\uparrow d_\downarrow u_\uparrow\rangle) + \text{perm.}, \tag{19}$$

where "perm." means the sum over all quark permutations and f_N is the overall normalization constant not needed for our calculation. The neutron wave function is obtained by interchange $d \leftrightarrow u$. As we can see, the distribution amplitude is completely determined by the function ϕ_1.

In general, the distribution amplitude and thus ϕ_1 depend logarithmically on Q^2. Namely, we have

$$\phi_1(x_i, Q^2) = x_1 x_2 x_3 \sum_k [\alpha_s(Q^2)]^{\gamma_k} B_k P_k(x_1, x_3), \tag{20}$$

where P_k are Appell polynomials ($P_1 = 1$, $P_2 = x_1 - x_3$, etc.) and γ_k are corresponding anomalous dimensions [15]. Thus in the formal limit $Q^2 \to \infty$ the term with the lowest γ_k, which is P_1, dominates and $\phi_1 \to \phi_{as} = x_1 x_2 x_3$. This asymptotical wave function, however, leads to predictions inconsistent with the experiment. In particular, it yields zero proton and positive neutron magnetic form factors. Thus at present Q^2 the distribution amplitude should be considerably different from its asymptotic form [16]. Since the evolution with Q^2 is very slow ($\gamma_k \ll 1$), the same wave function can be employed for all currently accessible Q^2 with reasonable accuracy.

Various forms of distribution amplitude were proposed in the literature. We did the calculations with the following amplitudes: Chernyak-Zhitnitsky (CZ) [16], King-Sachrajda (KS) [17], Chernyak-Ogloblin-Zhitnitsky (COZ) [18], Gari-Stefanis (GS) [19], and heterotic (Het) [20]. The CZ and KS amplitudes give practically the same results as the COZ amplitude, thus they are not considered further.

IV. NUMERICAL RESULTS

There are two independent kinematical variables in any elastic process. For eN scattering, Q^2 and ε [Eq. (3)] are generally used. The ε dependence of the obtained TPE amplitude $\delta\mathcal{G}_M$ is shown in Fig. 2. It turns out to be universal for all Q^2 (except for slow logarithmic evolution, which we neglect here). We see that the amplitude $\delta\mathcal{G}_M$, calculated with COZ and Het wave functions, is very close to a linear function of ε. Slight deviations from linearity are present near the endpoints $\varepsilon = 0$, $\varepsilon = 1$ only. In contrast, the GS wave function yields a much larger and highly nonlinear TPE amplitude. In light of this it is worth noting that linear ε dependence of $\delta\mathcal{G}_M$ is necessary and sufficient for Rosenbluth plots to remain linear even under the influence of TPE [21]. Since a careful analysis of the experimental data does not reveal any nonlinearity in the Rosenbluth plots [22], we conclude that the experiment disfavors the GS wave function.

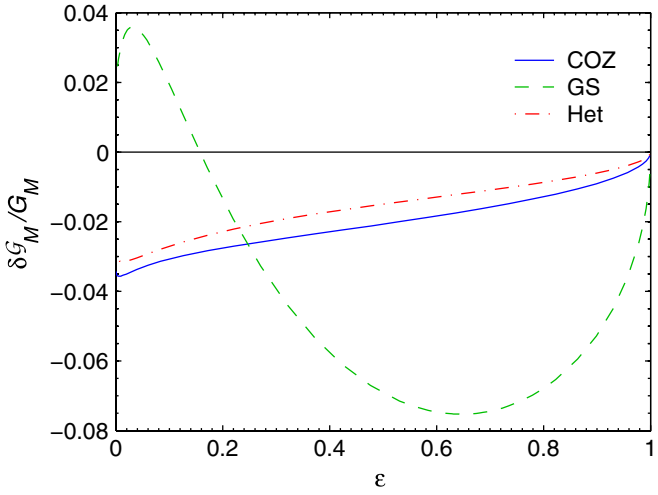

FIG. 2 (color online). TPE amplitude $\delta\mathcal{G}_M/G_M$ vs ε at $Q^2 = 10$ GeV^2.

For the neutron target, both GS and Het wave functions yield nonlinear and anomalously huge TPE corrections, up to 25% (Fig. 3). Taking into account the smallness of the

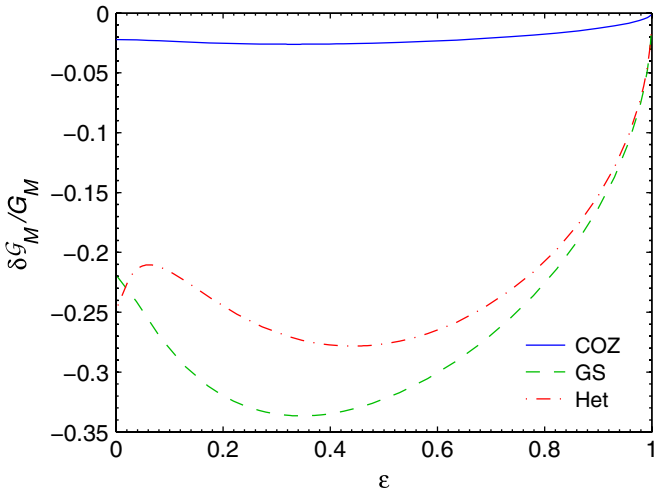

FIG. 3 (color online). TPE amplitude $\delta\mathcal{G}_M/G_M$ vs ε for neutron at $Q^2 = 5$ GeV^2.

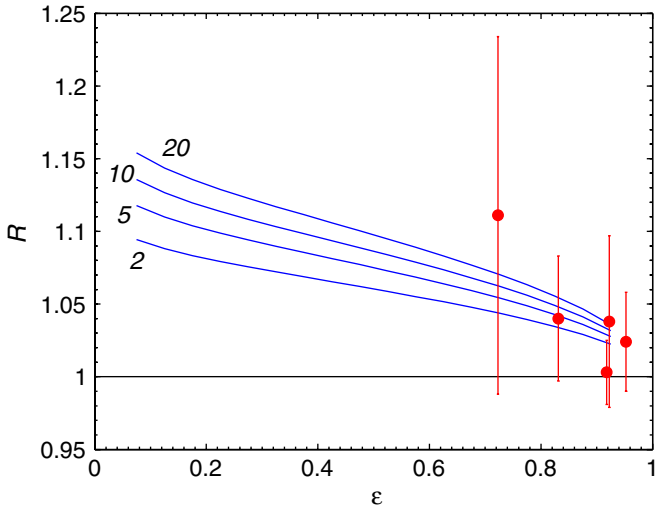

FIG. 4 (color online). Positron/electron cross section ratio for $Q^2 = 2$, 5, 10, and 20 GeV^2 (shown near the curves). Data are from Ref. [23] at $1.5 < Q^2 < 5$ GeV^2.

neutron electric form factor, these corrections would manifest as severe nonlinearities of the Rosenbluth plots, that is, strong ε dependence of the elastic cross section. Though such cross section behavior seems unlikely, the high-Q^2 neutron form factor data are too poor to draw a final conclusion. Further experimental study of electron-neutron elastic scattering at high Q^2 and different ε can show definitely whether the nucleon is described by Het or by COZ wave function. For the present moment we take the COZ wave function as the most plausible.

The amplitude $\delta\mathcal{G}_3$, which determines the correction to longitudinal recoil polarization [Eq. (7)], is small ($< 1\%$) for both proton and neutron, and unfortunately lies below the precision of today's experiments.

The positron/electron cross section ratio is shown in Fig. 4. The calculation is done with the COZ wave function at $Q^2 = 2$, 5, 10, and 20 GeV^2. The experimental data in the range $1.5 < Q^2 < 5$ GeV^2 from Ref. [23] are also shown. Though the data points are well near the curves, the errors are very large. More precise data would be helpful, preferably in the low-ε region, where the predicted ratio is higher.

The Q^2 dependence of "normalized" TPE amplitudes at fixed ε is completely determined by the evolution of a strong coupling constant α_s. We have used simple parameterization

$$\alpha_s = 4\pi/[\beta \ln(Q^2/\Lambda^2)], \tag{21}$$

with $\Lambda = 0.2$ GeV. The resulting shape of the TPE amplitude $\delta\mathcal{G}_M$ for the proton, calculated with the COZ wave function, is plotted in Fig. 5. At $Q^2 \approx 30$ GeV^2, which is today the maximal Q^2 ever investigated, the relative value of TPE amplitude reaches 3.5%, which corresponds to the cross section correction of about 7%. Such a correction is, however, smaller than the experimental errors. On the other hand, TPE can be seen in the recently proposed high-Q^2 JLab experiment [9], where the estimated errors are at the 1% level.

The results of the hadronic calculation [11,13] are also shown in Fig. 5 for comparison. Probably, the amplitude undergoes some gradual transition from this curve at lower Q^2 to pQCD prediction at higher Q^2 (recall that ε dependence in both cases is the same, approximately linear with the positive slope). The figure suggests that a reasonable interpolation is possible between the hadronic result for Q^2 below ~3 GeV^2 and the pQCD result above this value. But we also see a strong disagreement of these two curves at higher Q^2. The most likely reason for such behavior is that the hadronic approach, i.e. saturation of the intermediate hadronic states by the bare nucleon and the lowest resonances, is inadequate at high Q^2. The multi-

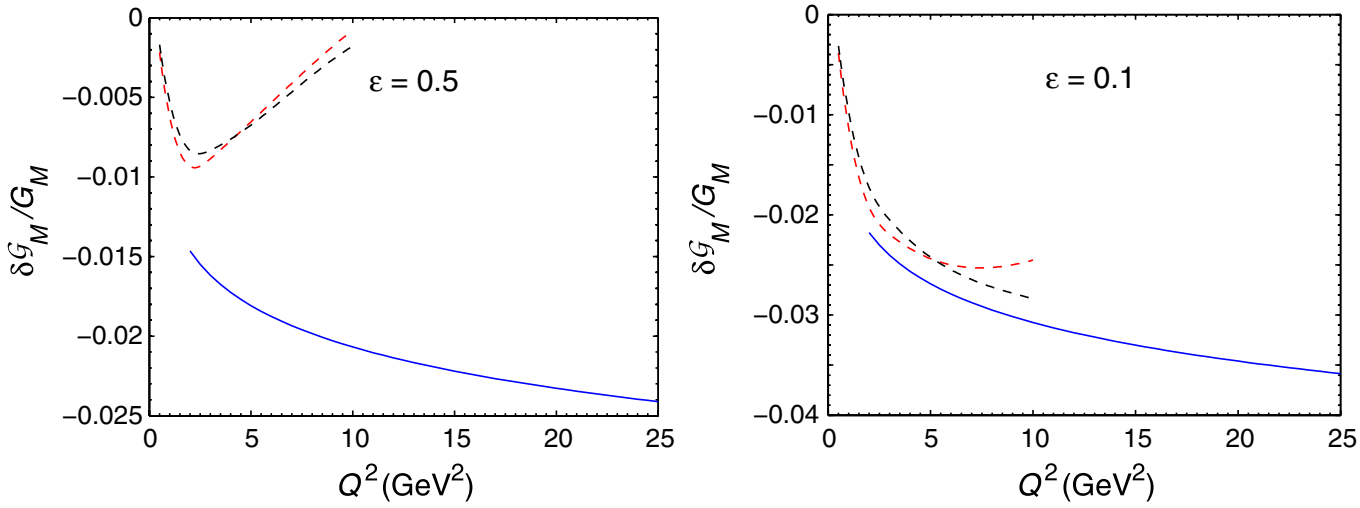

FIG. 5 (color online). TPE amplitude $\delta\mathcal{G}_M$ vs Q^2 at $\varepsilon = 0.5$ (left) and $\varepsilon = 0.1$ (right). Dashed curves show hadronic calculations, with form factors' parameterizations: dipole (red) and Ref. [24] (black).

particle intermediate states yield a substantial part of the amplitude.

V. CONCLUSIONS

We have considered TPE for the elastic electron-nucleon scattering in the framework of pQCD. The calculations are done in the leading order with several model wave functions. For the proton target and wave functions based on quantum chromodynamics sum rules (CZ [16], KS [17], and COZ [18]), the TPE amplitude $\delta\mathcal{G}_M$, which determines cross section correction, has linear ε dependence. Its value is of order α/α_s, grows logarithmically with Q^2, and at $Q^2 = 30$ GeV^2 reaches 3.5% of the Born amplitude. At lower Q^2 a smooth connection is possible with previous hadronic calculations, in which TPE amplitudes were calculated taking into account just the nucleon intermediate state [11]. On the other hand, at high Q^2 the results of these two methods are very different, which implies that the hadronic approach becomes inadequate at $Q^2 \gtrsim 3$ GeV^2.

The size and ε dependence of TPE amplitudes are sensitive to the choice of nucleon wave function (quark distribution amplitude). At the same time, they are directly measurable: $\delta\mathcal{G}_M/G_M$ via the cross section or the positron/electron cross section ratio and $\delta\mathcal{G}_3/G_M$—via the longitudinal recoil polarization. Thus an accurate measurement of TPE observables opens a new efficient way to study quark distribution amplitude in the nucleon. For example, the existing experimental data already rules out the GS wave function (Ref. [19]). Since TPE amplitudes have nontrivial ε dependence, they potentially provide much more information than just nucleon form factors. Thus TPE turns from the correction to form factor measurements into an independent tool for studying nucleon structure.

ACKNOWLEDGMENTS

This work was supported by the Program of Fundamental Research of the Department of Physics and Astronomy of the National Academy of Sciences of the Ukraine, and by the Ukraine State Foundation for Fundamental Research under Grant No. F16-458-2008.

[1] J. Arrington, Phys. Rev. C **68**, 034325 (2003).
[2] P. G. Blunden, W. Melnitchouk, and J. A. Tjon, Phys. Rev. C **72**, 034612 (2005).
[3] Measurement of the Two-Photon Exchange Contribution in ep Elastic Scattering Using Recoil Polarization (JLab experiment E04019), Spokespersons: R. Gilman, L. Pentchev, C. Perdrisat, and R. Suleiman; Beyond the Born Approximation: A Precise Comparison of Positron-Proton and Electron-Proton Elastic Scattering in CLAS (JLab experiment E04116), Spokespersons: A. Afanasev, J. Arrington, W. Brooks, K. Joo, B. Raue, and L. Weinstein; A Measurement of Two-Photon Exchange in Unpolarized Elastic Electron-Proton Scattering (JLab experiment E05017), Spokesperson: J. Arrington.
[4] S. P. Wells *et al.*, Phys. Rev. C **63**, 064001 (2001); F. E. Maas *et al.*, Phys. Rev. Lett. **94**, 082001 (2005).
[5] P. G. Blunden and I. Sick, Phys. Rev. C **72**, 057601 (2005).
[6] A. V. Afanasev and C. E. Carlson, Phys. Rev. Lett. **94**, 212301 (2005).
[7] A. Afanasev, M. Strikman, and C. Weiss, Phys. Rev. D **77**, 014028 (2008).
[8] Measurement of G_{Ep}/G_{Mp} to $Q^2 = 9$ GeV^2 via recoil polarization (JLab experiment E04108), Spokespersons: E. Brash, M. Jones, C. Perdrisat, and V. Punjabi.
[9] Precision Measurement of the Proton Elastic Cross Section at High Q^2 (JLab experiment E1207108), Spokespersons: S. Gilad, B. Moffit, B. Wojtsekhowski, and J. Arrington.
[10] Measurement of the Neutron Magnetic Form Factor at High Q^2 Using the Ratio Method on Deuterium (JLab experiment E1207104), Spokespersons: W. D. Brooks, G. Gilfoyle, K. Hafidi, and M. Vineyard.
[11] D. Borisyuk and A. Kobushkin, Phys. Rev. C **74**, 065203 (2006).
[12] S. Kondratyuk and P. G. Blunden, Phys. Rev. C **75**, 038201 (2007).
[13] D. Borisyuk and A. Kobushkin, Phys. Rev. C **78**, 025208 (2008).
[14] A. Afanasev, S. J. Brodsky, C. E. Carlson, Y. C. Chen, and M. Vanderhaeghen, Phys. Rev. D **72**, 013008 (2005).
[15] G. P. Lepage and S. J. Brodsky, Phys. Rev. D **22**, 2157 (1980). The expression for nucleon form factor in this paper the has wrong overall sign.
[16] V. L. Chernyak and A. R. Zhitnitsky, Phys. Rep. **112**, 173 (1984).
[17] I. D. King and C. T. Sachrajda, Nucl. Phys. **B279**, 785 (1987).
[18] V. L. Chernyak, A. A. Ogloblin, and I. R. Zhitnitsky, Yad. Fiz. **48**, 841 (1988).
[19] M. Gari and N. G. Stefanis, Phys. Rev. D **35**, 1074 (1987).
[20] N. G. Stefanis and M. Bergmann, Phys. Rev. D **47**, R3685 (1993).
[21] D. Borisyuk and A. Kobushkin, Phys. Rev. C **76**, 022201 (R) (2007).
[22] V. Tvaskis *et al.*, Phys. Rev. C **73**, 025206 (2006).
[23] J. Mar *et al.*, Phys. Rev. Lett. **21**, 482 (1968).
[24] J. Arrington, W. Melnitchouk, and J. A. Tjon, Phys. Rev. C **76**, 035205 (2007).